Molecular Architecture of the Mutagenic Active Site of Human Immunodeficiency Virus Type 1 Reverse Transcriptase: Roles of the β8-αE Loop in Fidelity, Processivity, and Substrate Interactions†

Kellie K. Weiss,‡ Seth J. Isaacs,‡ Nancy H. Tran,‡ Elinor T. Adman,§ and Baek Kim*,‡

Department of Microbiology and Immunology, University of Rochester Medical Center, 601 Elmwood Avenue, Box 672, Rochester, New York 14642, and Department of Biological Structure, University of Washington, Seattle, Washington 98195

Received April 7, 2000; Revised Manuscript Received June 29, 2000

ABSTRACT: Human immunodeficiency virus type 1 (HIV-1) reverse transcriptase (RT) is a putative source of the genomic hypermutation that promotes rapid evolution of HIV-1. To understand the molecular strategies that create a highly mutagenic DNA polymerase active site in HIV-1 RT, we investigated the roles of four residues in the β8-αE loop. Gln151, which interacts with the sugar of the incoming dNTP, and Lys154, which interacts with the template, yielded site-directed mutants with increased fidelity, suggesting that these residues are directly involved in the mutagenic architecture of the active site. Mutations at Gln151 and Lys154 also reduced processivity. Q151N RT showed enhanced ability to discriminate between TTP and AZT triphosphate, consistent with the observation that the Q151M mutation confers AZT resistance in vivo. Mutations at Gly152 greatly decreased RT activity; molecular modeling suggests that Gly152 is critical for the proper geometric alignment that permits base-paring of the incoming dNTP with the template. Mutations at Trp153 reduced the expression level, and presumably the stability, of RT proteins in bacteria. These observations support the conclusion that interactions of active site residues in the β8-αE loop with incoming dNTPs and the template are determinants of the accuracy, processivity, and substrate selectivity of HIV-1 RT.

In most organisms, synthesis of mutations during replication of the genome is prevented both by the accuracy of the replication machinery and by efficient repair mechanisms. In contrast, some organisms that employ a high level of mutation synthesis for their evolutionary advantage, such as human immunodeficiency virus type 1 (HIV-1),[1] contain error-prone replication machinery and lack repair mechanisms. Indeed, HIV-1 reverse transcriptase (RT) is the most unfaithful DNA polymerase known (*1*, *2*), and this infidelity is a putative source of HIV-1 diversity and evolution (*3*, *4*).

Lack of a 3′ → 5′ proofreading exonuclease is an important factor contributing to the inaccuracy of HIV-1 RT (*2*). However, other viral RTs that lack proofreading activity, such as MuLV RT and AMV RT, have 10−18 times higher fidelity than HIV-1 RT (*5*). This suggests that additional mechanisms contribute to the infidelity of HIV-1 RT. The structural and mechanistic bases of HIV-1 RT infidelity remain to be fully elucidated.

Mutants with altered fidelity are invaluable in delineating the structural and biochemical determinants of replicational accuracy, as illustrated by studies of the Klenow fragment (KF) of *E. coli* DNA polymerase I (*6*) and the corresponding fragment (Klentaq1) of the highly homologous, thermostable *Thermus aquaticus* DNA polymerase I (Taq Pol, *7*). For example, in cocrystal structures of KF and Klentaq1 complexed with DNA, four conserved amino acids located in the O-helix near the finger domain face toward the substrate binding cleft (*8*). Biochemical and mutagenesis studies indicate that three of these amino acids may interact with the incoming dNTP, and in recent crystal structures of Klentaq1 complexed with DNA and a dNTP, these residues are indeed found to directly contact the dNTP (*9*). Importantly, mutation of one of these amino acids in *E. coli* DNA polymerase I, namely, R754, has been shown to confer an anti-mutator phenotype (*6*), suggesting that interactions with the incoming dNTP are a potential determinant of the accuracy of DNA polymerization. Moreover, mutation in several O-helix residues of Taq Pol has been shown to reduce fidelity (*7*). HIV-1 RT does not have an O-helix-like dNTP binding site. A recent crystal structure shows that numerous residues in the finger and palm domains, such as K65, R72, L74, A114, Y115, Q151, and D113, interact with incoming dNTPs (*10*). Mutations in many of these residues, e.g., Q151M, arise when the virus is grown under selection with

† This work was supported by National Institutes of Health (NIH) Grant R29-GM55500 to B.K. Structure modeling was supported by the National Institute of Environmental Health Sciences, NIH Grant P30-ES07033 Facility Core 5, Molecular Structure Visualization to E.T.A.

* Correspondence should be addressed to this author at the Department of Microbiology and Immunology, 601 Elmwood Ave., Box 672, University of Rochester Medical Center, Rochester, NY 14672. Tel: (716) 275-6916, Fax: (716) 473-9573, E mail: baek_kim@urmc.rochester.edu.

‡ University of Rochester Medical Center.

§ University of Washington.

[1] Abbreviations: dNTP, 2′-deoxynucleoside 5′-triphosphate; AZT, 3′-azodithymidine; AZTTP, 3′-azidothymidine 5′-triphosphate; T/P, template-primer complex; p66, 66 kDa RT polypeptide; SDS, sodium dodecyl sulfate; DDDP, DNA-dependent DNA polymerase; RDDP, RNA-dependent DNA polymerase.

10.1021/bi000788y CCC: $19.00
Published on Web 08/04/2000

nucleoside inhibitors of RT, such as AZT (*11*, *12*), and confer resistance to the inhibitors. Interestingly, the Q151M mutation also alters mutational specificity (*13*). These findings suggest that interactions of HIV-1 RT with incoming dNTPs may affect the selectivity for both dideoxynucleotide analogues and natural dNTPs.

Structural and mutational analyses also suggest that interactions of DNA polymerases with template nucleotides may contribute to replicational accuracy. In the case of KF and Klentaq1, for example, a conserved tyrosine at the carboxyl terminus of the O-helix stacks against the first template nucleotide of the duplex portion of the template-primer. Mutations at this residue in KF, namely, Y766A and Y766S, result in reduced fidelity (*14*). In the case of HIV-1 RT, we have shown that mutations at D76 and R78 in the β3-β4 finger domain, confer large (9-fold) increases in accuracy (*15*, *16*). As proposed in a recent crystallographic study (*10*), and in our earlier model (*16*), these residues lie near the template nucleotide that base-pairs with incoming dNTPs. Presumably, interactions of D76 and R78 with this nucleotide may contribute to the creation of a mutagenic active site where mispairing can readily occur. Another HIV-1 RT mutation that increases accuracy, E89G (*17*), may also affect fidelity via altered interactions with the template, since structural modeling suggests that E89 interacts with the penultimate nucleotide of double-stranded RNA or DNA templates.

The crystal structure of HIV-1 RT complexed with DNA and dNTP (*10*) shows that three of four contiguous amino acids in the β8-αE loop, namely, Q151, G152, W153, and K154, interact with either the incoming dNTP and/or a template nucleotide. Q151 interacts with the sugar of the incoming dNTP, and G152 interacts with both the base and sugar moieties of the template nucleotide that base-pairs with the incoming dNTP. K154 interacts with the phosphate group of the template nucleotide that base-pairs with the nucleotide at the 3′ end of the primer, while W153 interacts with neither the dNTP nor the template. Based on these observations, and on the premise that interactions of DNA polymerases with both dNTPs and template nucleotides can be determinants of replicational accuracy, we sought to produce fidelity mutants by site-directed mutagenesis targeting these four residues. We report here a new set of HIV-1 RT mutants with greatly enhanced fidelity that also display altered processivity and drug resistance. We discuss the roles of HIV-1 RT interaction with the incoming dNTP and with the template in fidelity, substrate selectivity, and processivity.

MATERIALS AND METHODS

Strains and Plasmids. E. coli NM522 (Stratagene, CA) was used for construction of plasmids, and BL21 (Novagen, WI) for overexpression of HIV-1 RT. pBK33 is pHis/*Nde*I (from Dr. A. Hizi) encoding full-length wild-type p66 HIV-1 RT, fused at the N-terminus to six histidine residues (*18*, *19*).

Construction of HIV-1 RT Mutants. Amino acid substitutions at four residues (Q151, G152, W153, and K154) of HIV-1 RT were individually generated by using PCR-based site-directed mutagenesis with four different primers [5′-AAAAAAGGATCC TTT(K154) CCA(W153) TCC(G152) TTG(Q151) CCTGTGGAAGCA CATTATACTGATATC-3′) encoding (−) strand sequences of the β8-αE region of HIV-1 RT. These primers contained mutations at the positions encoding each of the four residues underlined, and a *Bam*HI site at position 155. Both sequences at K154 (TTT) and W153 (CCA) positions were mutated to A(G+T)(C+A), giving Asp, Ala, Ser, and Tyr mutations. The sequence at G152 (TCC) was mutated to A(G+T)(C+A+T), giving Asp, Ala, Ser, Tyr, Thr, and Asn mutations. The sequence at Q151 (TTG) was mutated to (A+T)TT, giving Asn and Lys mutations. The products of PCR amplification with each of the four primers and the 5′ SD RT primer that encodes the N-terminal sequence of HIV-1 RT and the *Nde*I site (*18*), were inserted into pBK33 for p66 RT after digestion with *Nde*I and *Bam*HI. A 465 bp region between *Nde*I and *Bam*HI of the plasmids was sequenced by the ABI system to confirm mutations at positions 151−154.

Purification of HIV-1 RT. Procedures for purification of the hexahistidine-tagged p66 and p51 monomers of HIV-1 RT by Ni^{2+} chelation chromatography have been described (*19*). Amounts of purified monomers were estimated in the Bradford assay (BioRad, Richmond, CA) with a bovine serum albumin standard; most of the preparations were of >95% purity, estimated by visual inspection of Coomassie Blue-stained SDS−polyacrylamide gels. We previously found that 6-His tag of purified HIV-1 RT proteins does not affect DNA polymerase activity and sensitivity to a nucleotide analogue (*18*). We also previously reported that both p66/p51 heterodimers and p66/p66 homodimers of wild-type and mutant HIV-1 RT proteins showed the same level of misincorporation in four different types of primer extension reactions (*15*, *16*). With this protocol, in most of the HIV-1 RT proteins, we were able to purify 2 mg of RT proteins with greater than 95% purity from 1 L of culture. However, expression levels of two W153 mutants, W153A and W153S, were low, and concentrations of these prepared RT mutant proteins were 8−10 times lower than those of wild-type HIV-1 RT, and their protein purity was 90%.

Determination of Specific Activity of Purified RT Proteins. Three templates were used to measure both DDDP and RDDP activities of RT proteins. The heterogeneous DNA template is a gapped salmon sperm DNA prepared as described (*20*). The homogeneous RNA template-primer is poly(rA) (286−428 nt long, Amersham-Pharmacia, NJ) annealed to 20 bp long oligodT (Amersham-Pharmacia, NJ). The heterogeneous RNA template-primer is 40 nt long RNA with heterogeneous sequence (see below for misincorporation assay) annealed to 17-mer DNA primer (see below). Reaction mixtures (20 μL) contained 50 nM HIV-1 RT, dNTPs (100 μM each), ^{3}H-TTP (10 μM, ICN), 25 mM Tris-HCl (pH 8.0), 100 mM KCl, 2 mM DTT, 5 mM $MgCl_2$, 0.1 mg/mL bovine serum albumin, and either gapped salmon sperm DNA (5 μg), poly(rA)/oligodT (1 μg), or heterogeneous RNA-annealed 17-mer DNA (100 ng). Reactions were incubated at 37 °C for 5 min and terminated by addition of 400 μL of 10% TCA. The incorporation of ^{3}H-TTP was linear up to 15 min incubation time under this condition. The protocol for this assay was previously described (*15*, *16*).

Primer Extension Assay with DNA or RNA Templates (Misincorporation Assay). Procedures were modified from those of Preston et al. (*1*). The DNA template-primer was prepared by annealing a 63-mer (5′-TAATACGACTCAC-TATAGGGAGGAAGCTTGGCTGCAGAATAT-

TGCTAGCGGGAATTCGGCGCG-3′) to a 17-mer (5′-CGCGCCGAATTCCCGCT-3′) ^{32}P-labeled at the 5′ end with T4 polynucleotide kinase (template:primer, 2.5:1). The RNA template-primer was also prepared by annealing a 40-mer (5′-AAGCUUGGCUGCAGAAUAUU UGCUAGCGGGAAUUCGGCGCG-3′, Dharmacon Research, CO), which encodes the same sequence as the 3′ part of the 63-mer DNA template, to the 17-mer used for DNA template-primer preparation. Assay mixtures (20 μL) contained 10 nM template-primer, 20−100 nM HIV-1 RT as specified in the figure legends, 3 or 4 dNTPs (250 μM each), 25 mM Tris-HCl (pH 8.0), 100 mM KCl, 2 mM DTT, 5 mM $MgCl_2$, 2 μM $(dT)_{20}$, and 0.1 mg/mL bovine serum albumin. Two protein concentrations (4× and 1×) of wild type (20 and 5 nM), Q151N (40 and 10 nM), and Q151K (60 and 15 nM) were used in RNA template reactions (Figure 2), and two concentrations (4× and 1×) of wild type (40 and 10 nM) and Q151 (60 and 15 nM) were used for DNA template reactions (Figure 3A). Two concentrations (2× and 1×) of wild type (20 and 10 nM) and K154A (50 and 25 nM) were used for DNA template reactions (Figure 3B). Reactions were incubated at 37 °C for 5 min and terminated by 4 μL of 40 mM EDTA, 99% formamide. Reaction products were immediately denatured by incubating at 95 °C for 3 min and analyzed by electrophoresis in 14% polyacrylamide−urea gels.

Extension of Mismatched Primers. To measure RT's capability to extend mismatched primer, we used two different mismatched primers annealed to either RNA or DNA template used in the misincorporation assay. G/T mismatched primer (5′-CGCGCCGAATTCCCGT-3′) was annealed to the 40-mer RNA template (see above) with G/T mismatched at the 3′ end nucleotide underlined. C/A mismatched primer (5′-CGCGCCGAATTCCCGCTAA-3′) was annealed to the 63-mer DNA template (see above) with the C/A mismatch at the 3′ end nucleotide underlined. The extension condition for these mismatched primers was the same as the one for misincorporation described above except for RT concentrations and T/P. The same RT activities of wild type and Q151N mutant proteins were used in this assay, as determined by the extension reaction with matched A primer. Two RT concentrations (2× and 1×) of wild type (80 and 40 nM) and Q151N (160 and 80 nM) were used in this assay. The minus dCTP and minus dGTP biased dNTP pools were used for G/T and C/A mismatched primer extension reactions, respectively. Possible removal of the mismatched primer nucleotides during the reaction could generate one nucleotide shorter matched primers that can be extended and contaminate the true products directly extended from the mismatched ends. Use of the biased dNTP pools minimizes extension of these degraded matched primers or one nucleotide shorter primer originally contaminated in synthesized oligomers. The reactions were also analyzed by a 14% denaturing gel.

M13mp2 lacZ Forward Mutation Assay. The mutation frequencies for wild-type and mutant HIV-1 RTs were measured essentially as previously described (*21*). M13mp2 DNA containing a 361-nucleotide single-stranded gap was prepared as specified (*21*). Gapped M13mp2 DNA (1 μg) was incubated with RT (100−500 nM) at 37 °C for 20 min under the conditions described above for the misincorporation assays. The extended gapped DNAs by equal total DNA polymerase activities of wild-type (100 nM) and mutant proteins (250 nM) were analyzed by 0.7% agarose for checking the production of double strand M13 DNA with filled gaps (*21*). The extended gapped DNAs were transformed to MC1016 cells, and the transformed cells were plated to M9 plates containing X-gal and IPTG with CSH50 lawn cells. The mutation frequency was determined as the ratio of mutant (pale blue and white) plaques to mutant plus wild-type (dark blue) plaques as described (*21*).

Processivity Assay. The reaction condition for measuring processivity requires a single round of primer extension (*16*). RT proteins were preincubated with 10 nM poly(rA) (average size = 260 nt, Amersham-Pharmacia, NJ) annealed to the ^{32}P-labeled 20-mer oligodT (Amersham-Pharmacia, NJ) or 1 μg of single-strand DNA of phage M13mp18 annealed to 20 nM 24-mer M13 sequencing primer (New England Biolabs, MA) for 3 min at 20 °C. The concentrations of wild type, Q151N, Q151K, and K154A for poly(rA) reactions were 10 nM, 40 nM, 200 nM, and 15 nM, respectively. For M13 ss DNA template, the concentrations of wild type, Q151N, and K154A were 20 nM, 50 nM, and 50 nM, respectively. The extension reactions were initiated by adding the trap mixture containing dNTPs (0.5 mM with a final concentration of 5 mM $MgCl_2$), molar excess of cold poly(rA)/oligodT (4 μg/20 μL), and heparin (10 μg/20 μL). The extension reactions were terminated by 4 μL of stop solution after 3 min incubation at 37 °C. Control reactions were performed as described (*16*), confirming the single round of primer extension under this reaction condition. The terminated processivity reaction and control reactions were analyzed by 11% polyacrylamide−urea after 3 min heat inactivation.

Sensitivity of RT Proteins to a Dideoxynucleotide Chain Terminator, AZTTP. The assay for sensitivity of RT proteins to chain terminators was the primer extension assay with mixtures of natural dNTPs (200 μM) and AZTTP (100 μM; Moravek, CA). Less total RT activities of the mutant proteins (Q151N, 30 nM, and Q151K, 30 nM, in RNA template reactions, and Q151N, 75 nM, in DNA template reactions) than that of wild-type HIV-1 RT (20 nM in RNA template reactions and 40 nM in DNA template reactions) were used to verify that less inhibition of mutant protein by AZTTP is not due to more RT activities of the mutant proteins used. The reaction condition for this assay was the same as described in the misincorporation assay except for dNTP pools. Both RNA and DNA templates were used for Q151N and wild-type proteins, but only RNA template was used for Q151K due to large reduction of DDDP activity in the Q151K mutant. The reactions were analyzed in a 14% polyacrylamide−urea gel.

RESULTS

HIV-1 RT Mutants Containing Mutations between Residues 151 and 154, and Their RT Activities. Four HIV-1 RT residues between amino acids 151 and 154 were individually targeted by PCR-based site-directed mutagenesis (Figure 1A). The residues in the β8-αE target region of HIV-1 RT provide various interactions with template nucleotides and the incoming dNTP (Figure 1B). Each of four positions was mutated to more than two different mutations (Figure 1A). Mutant and wild-type HIV-1 RT proteins were purified from

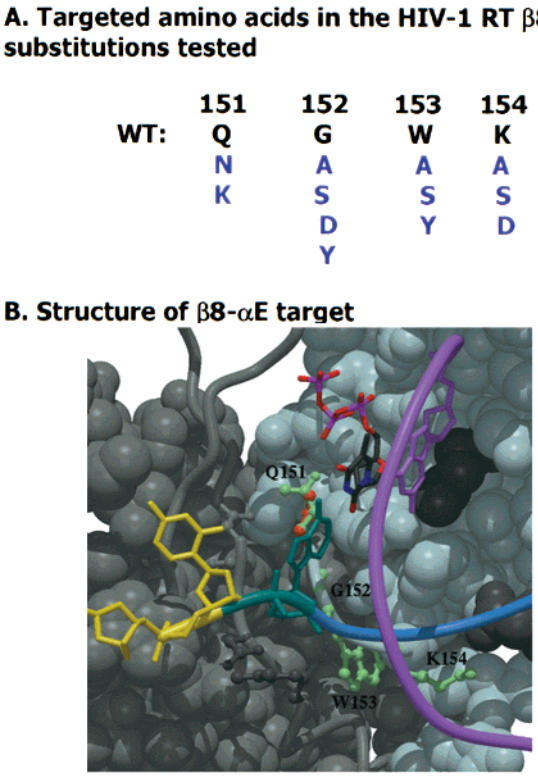

FIGURE 1: Target sequence of the HIV-1 RT β8-αE region and constructed mutations (A) and structure of HIV-1 RT near the target region (B). (A) Wild-type sequences of the target amino acid residues at each position are shown next to WT. Mutations (blue) generated at each of four residues are shown under each of the wild-type sequences (black). (B) Four target residues (Q151, G152, W153, and K154) are light green. Primer (purple), double-stranded part of the template (light blue) base-paired to the primer, single-stranded part of the template (yellow), and the template nucleotide (blue-green) base-pairing to the incoming dNTP (black-red) are also shown. Coordinates for the figure are from PDB file 1rtd (*10*, *32*). The figure was drawn using Molscript (*33*) and Raster3D (*34*).

an *E. coli* overexpression system by using a Ni^{2+} affinity purification system. We examined DNA- and RNA-dependent DNA polymerase (DDDP and RDDP) activities of purified RT proteins using one DNA template with a heterogeneous sequence and two RNA templates with either homogeneous poly(rA) or heterogeneous sequences. The percent of specific activities of the mutants relative to that of wild-type HIV-1 RT was determined (Table 1). Interestingly, none of the four G152 mutants were active, indicating that the G152 residue is essential for RT activity. Two Q151 mutants, Q151N and Q151K, showed different template preference. Q151N showed more than 24% of wild-type RT activities with all three kinds of template, whereas Q151K maintained only high RDDP activity with heterogeneous RNA template. In the reactions with poly(rA) template, one of the most preferred templates of wild-type HIV-1 RT, Q151N still has considerable RDDP activity, whereas Q151K totally lost RDDP activity. Two mutants of W153 changed to the amino acids with smaller R groups (serine and alanine) showed low RT activities in all three templates tested, whereas W153Y mutant has 19−25% of wild-type activities. Two K154 mutants, K154A and K154S, showed 35−79% of wild-type RT activities in all three templates, whereas K154E showed only 9−12% of wild-type activities. In general, Q151 and K154 HIV RT mutants maintained high levels of RDDP and DDDP activities.

Table 1: DDDP and RDDP Activities of RT Mutants Relative to Wild Type HIV-1 RT

HIV-1 RT target residues	mutations	% RT activity[a]		
		DNA template	RNA templates	
		heteropolymeric[b]	poly(rA)	heteropolymeric[c]
Q151	N	39	24	54
	K	5	4	30
G152	A	<2	<2	<2
	S	<2	<2	<2
	T	<2	<2	ND
	I	<2	<2	ND
W153	A	5	15	5
	S	7	12	10
	Y	19	25	22
K154	A	43	71	79
	S	35	51	61
	E	12	9	12

[a] Percent specific activity of wild-type HIV-1 RT protein was determined by incorporation of [^{3}H]-TTP as described (*18*). 1 unit of purified RT proteins is the amount of the enzyme that incorporates 1 nmol of [^{3}H]-TTP with different T/Ps for 10 min at 37 °C. Specific activities of purified wild-type HIV-1 RT protein were 8 [poly(rA)/oligodT], 1.5 (heteropolymeric DNA template), and 8 (heteropolymeric RNA template) units/μg, respectively. [b] Gapped salmon sperm DNA was prepared as described (*20*). [c] 40-mer RNA template annealed to 17-mer DNA template used for misincorporation assay (see Materials and Methods) was used.

Measurement of Fidelity of HIV-1 RT Mutants by Misincorporation Assay. We employed a misincorporation assay to compare the misincorporation capability of the five mutant RTs containing high RT activities (Q151N, Q151K, W153Y, K154A, and K154S) to that of wild-type HIV-1 RT. This assay is a primer extension assay that monitors both incorporation of incorrect dNTPs and extension of the mismatched primer by utilizing a synthetic DNA or RNA template-primer with biased dNTP pools containing only three kinds of dNTPs (*15*, *16*). In this assay, a higher

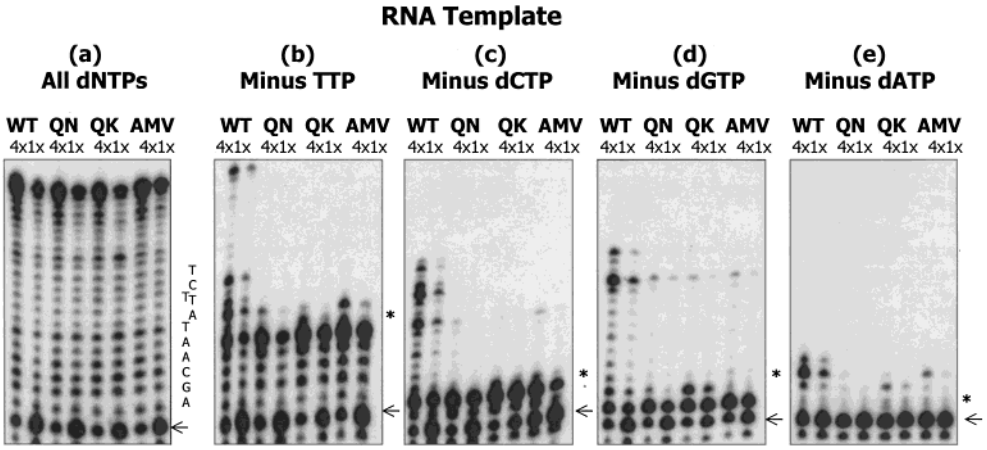

FIGURE 2: Misincorporation of RT proteins with heterogeneous RNA template. The ^{32}P-labeled 17-mer primer (arrow) annealed to 40-mer DNA template (5 nM) was extended by two different concentrations (4× and 1×) of wild-type (20 and 5 nM), Q151N (40 and 10 nM), and Q151K (15 and 60 nM) HIV-1 RT proteins, and AMV RT (0.2 and 0.05 units) at 37 °C for 5 min as seen in the extension reactions with all four dNTPs (a). The extension reactions were also performed in the presence of only three complementary dNTPs [(b) minus TTP, (c) minus dCTP, (d) minus dGTP, (e) minus dATP]. The extension reactions were analyzed by 14% denaturing gel electrophoresis. The DNA sequence of the first 11 nucleotides of the extended part of the primer is shown in (a). The sites with "*" indicate the first stop sites where the deleted dNTPs would be incorporated in the reactions with only three dNTPs. In this assay, the higher efficiency of elongation of terminated primer with only three nucleotides will reflect the lower fidelity of the HIV-1 RT protein assayed.

efficiency of primer extension will reflect a lower fidelity of the HIV-1 RT protein assayed.

A gel displaying extension of the 17-mer primer annealed to a 40-mer RNA template at two different concentrations (4× and 1×) of wild-type and two Q151 proteins is shown in Figure 2. We also employed AMV RT as a high-fidelity control RT. As shown in Figure 2a, in reactions containing all four dNTPs, the wild type, two Q151 mutant HIV-1 RTs, and AMV RT proteins catalyzed approximately the same amount of synthesis, leading to fully extended primers. When incubated with mixtures of only three dNTPs (Figure 2b: -TTP, 2c: -dCTP, 2d: -dGTP, 2e: -dATP), wild-type HIV-1 RT catalyzed substantial extension past nucleotides for which a complementary dNTP was deleted (see the sites with "*" in Figure 2, stop sites). The ability to incorporate incorrect nucleotides reflects the low-fidelity nature of wild-type HIV-1 RT. On the other hand, two Q151 mutants, Q151N and Q151K, catalyzed much less synthesis and therefore shorter extension than the wild-type enzyme in reactions with three dNTPs, indicative of higher replicational fidelity (Figure 2b−e). Interestingly, as seen in Figure 2b and e, both Q151N and Q151K mutants showed even more reduced levels of the primer extension than AMV RT, suggesting Q151 mutants have higher fidelity than AMV RT.

Next, we performed the misincorporation assay with a 63-mer DNA template. The sequence of the 40 nucleotides at the 3′ end of the 63-mer DNA template is the same as that of the 40-mer RNA template described above. In this assay, two different input levels of DNA-dependent DNA polymerase activities (4× and 1×) of wild-type and Q151N proteins were used (all four dNTPs in Figure 3A). As shown in Figure 3A with -TTP, Q151N extended less primer than wild-type HIV-1 RT in the presence of only three dNTPs, suggesting that Q151N mutants have a higher fidelity than wild type in the DDDP reaction. Reduced levels of the primer extension were also observed in the Q151N protein reactions containing -dCTP and -dGTP (data not shown). However, the misincorporation level of wild-type HIV-1 RT in the absence of dATP was too low to be compared with that of the mutant.

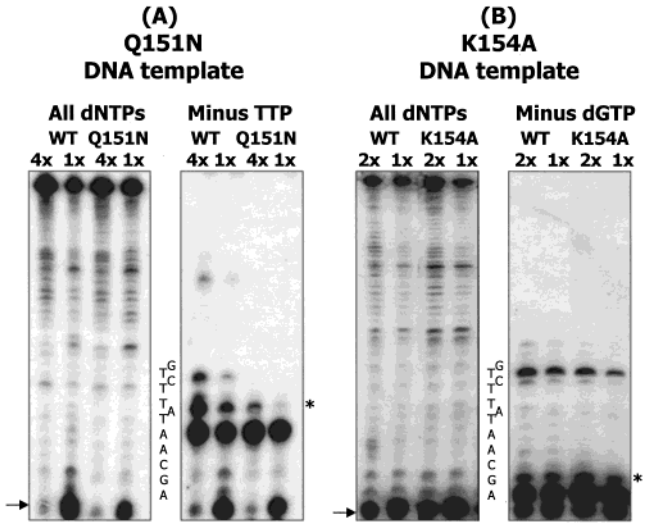

FIGURE 3: Misincorporation of Q151N (A) and K154A (B) RT proteins with heterogeneous DNA template. ^{32}P-labeled 17-mer primer annealed to the 63-mer DNA template was extended by two different total RT concentrations [4× for (A) or 2× and 1× for (B); see Materials and Methods] of wild-type and mutant HIV-1 RT proteins with all four dNTPs or three dNTPs [minus TTP for (A), minus dGTP for (B)]. Equal DDDP activities of RT proteins used in each set of the experiments were used as determined in the primer extension reactions with all dNTPs. Less total DDDP activity was used in the reactions with wild-type and K154A RT proteins (B) than those with wild-type and Q151N proteins (A). The DNA sequence of the first 12 nucleotides of the extended part of the primer is shown in the reactions with "All dNTPs". The sequence at the 3′ 40 nt region of the 63-mer DNA template was identical with that of the 40-mer RNA template used in Figure 2. Sites marked by an asterisk indicate the first stop sites generated due to deletion of the dNTP complementary to the template sequence. The primer remaining unextended is marked by arrows.

Two K154 mutants, K154A (Figure 3B) and K154S (data not shown), also showed slightly reduced levels of misincorporation in both the DNA and RNA template reactions lacking dGTP (Figure 3B), TTP, and dCTP. This suggests the K154A RT mutant could have slightly higher fidelity than wild-type HIV-1 RT. This small fidelity difference was

confirmed by multiple repeats of the assay. In the reaction with W153Y, the level of the misincorporated primer was not reduced (data not shown), suggesting that the W153Y mutant is not a hi-fi mutant.

Extension of Mismatched Primer by HIV-1 RT Proteins. Creation of one mutation during DNA synthesis consists of two different sequential steps: (1) incorporation of incorrect dNTP, and (2) extension of the mismatched primer generated by the misincorporation. In the misincorporation assay shown in Figures 2 and 3, extension of primer beyond the stop sites measured the capability of the RT proteins to misincorporate and then to extend upon the mismatched primer. Next, we examined the capability of wild-type and Q151N HIV-1 RT mutant proteins to extend the mismatched primer. In this study, we used two different mismatched primers (P) annealed to either RNA or DNA template (T). One T/P contains a G/T mismatch at the 3′ end of the primer annealed to the RNA template. The other T/P contains a C/A mismatch at the 3′ end of the primer annealed to the DNA template. These two mismatched T/Ps represent the replication intermediates that can be synthesized during the process of G to A mutation in the viral RNA sequence that is the most predominant HIV-1 mutation (*22*, *23*). We tested whether the Q151N mutant has a reduced capability to extend these two different mismatched T/Ps essential for creating the G to A mutation. The primer extension reactions were performed with only three dNTPs: -dCTP in the G/T mismatched primer reactions and -dGTP in the C/A mismatched primer reaction, to minimize contamination of the true product directly extended from the mismatched primer with the extension of one nucleotide shorter matched primer that could be generated by degradation of the mismatched primer during reaction. For this reason, we deleted the nucleotides that base-pair with template sequence at the mismatched sites (dCTP in G/T mismatch, and dGTP in C/A mismatch; see Figure 4B and C) in the dNTP pools. As seen in Figure 4A, in reactions containing only three dNTPs (-dGTP) and matched primer, both wild-type and Q151N proteins showed the same level of total primer extension (or remaining unextended primer). This suggests that the total RT activities of wild-type and mutant RTs added in this assay were the same. These reactions are identical with the ones shown in Figure 2D (-dGTP). In this control reaction, wild-type RT extended further beyond the stop site because of its lower fidelity than Q151N (see Figures 2 and 3). As seen in Figure 4B and C, the Q151N mutant protein showed a much lower level of primer extension from both the G/T and C/A mismatched primers than wild-type HIV-1 RT. These results suggest that the Q151N mutant has a reduced capability to extend the mismatched primer, which may contribute to enhancement of accuracy of DNA synthesis.

lacZ Forward Mutation Assay of HIV-1 RT Mutants. This method has been used to determine mutation frequencies in DDDP activities of DNA polymerases. Mutations generated when DNA polymerase or RT copies the gapped region of the *lac*Z gene in M13 mp2 can be scored by the number of plaques with altered color phenotype (pale blue or clear) in a specific indicator strain. Due to the large reduction of DDDP activity by the Q151K mutant, only wild type, Q151N, and K154A were used in this assay. As seen in Table 2, the Q151N HIV-1 RT mutant showed a 13-fold reduced mutation rate relative to the wild type HIV-1 RT; this

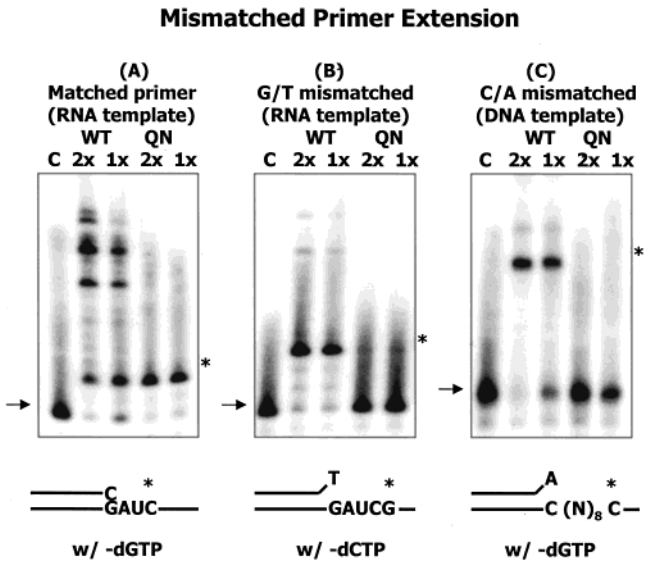

FIGURE 4: Extension of mismatched primer by HIV-1 RT proteins. ^{32}P-labeled 16-mer matched (A) and 16-mer G/T mismatched primers (B) were annealed to the 40-mer RNA template, and ^{32}P-labeled 19-mer C/A mismatched primer (C) was annealed to the 63-mer DNA template. The DNA sequences of the extended part of the primer are shown at the bottom of each gel. Equal RT activities of wild-type and Q151N mutant proteins determined with matched primer (A) were used in the reactions with mismatched primers. Biased dNTP pools allowing shorter primer extension were used for easier determination of primer extension beyond the mismatched sites. Stop sites due to deletion of the complementary dNTP are marked by (*). The primer extension condition in this assay was the same as described in the misincorporation assay (Figures 2 and 3) except for the RT concentrations (see Materials and Methods) and T/P. The unextended primers are shown as C and marked by arrows in each gel.

Table 2: M13 *lac*Z Forward Mutation Assay with Wild Type and Mutants

HIV-1 RT proteins	total plaques	mutant plaques	mutant frequency	fold decrease
wild type	11420	298	261	–
Q151N mutant	13520	27	20.0	×13
K154A mutant	10200	128	125	×2.1

mutation frequency was similar to those of AMV and MuLV RTs (*5*). The K154A mutant showed only a 2.1-fold decrease in error rate, which is consistent with the data obtained by the gel-based misincorporation assay (shown in Figures 2 and 3).

Processivity of HIV-1 RT Mutant Proteins. It has been shown that interaction of HIV-1 RT with the template affects its processivity (*24*). Since the residues in the β8-αE loop of HIV-1 RT lie near the single-stranded template, we tested the processivity of HIV-1 RT proteins using a poly(rA) template with which HIV-1 RT shows highest processivity. As seen in Figure 5A, Q151N mutants showed slightly reduced processivity (~200 nt) on the poly(rA) template, compared with wild-type HIV-1 RT (~250 nt). In addition, Q151N displays reduced processivity on a DNA template (Figure 5B). Q151K showed the most profound reduction in processivity (<10 nt) even with poly(rA) template. The observed processivity of Q151N on poly(rA) template is similar to the processivity of wild-type HIV-1 RT with poly-(dA) DNA template (<10 nt, *25*). K154A did not have altered processivity with poly(rA) template (Figure 5A),

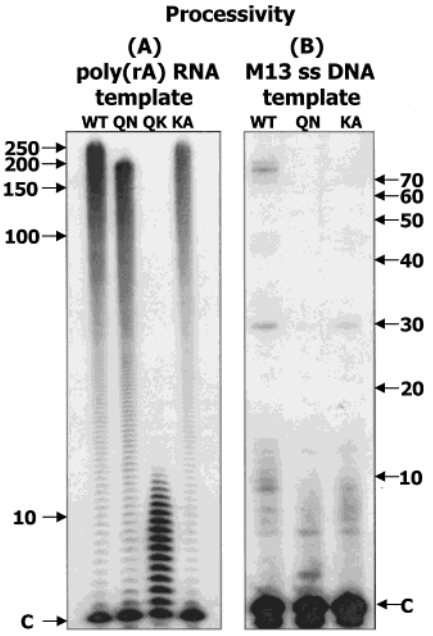

FIGURE 5: Processivity of HIV-1 RT proteins with RNA and DNA templates. Poly(rA) annealed to ^{32}P-labeled 20-mer oligodT [(A), RNA template] and M13 mp18 single-stranded DNA annealed to ^{32}P-labeled 20-mer forward primer [(B), DNA template] were used in this assay. QN, QK, and KA indicate Q151N, Q151K, and K154A HIV-1 RT mutant proteins. RNA (A) or DNA T/P (B) was first preincubated with RT proteins (WT, Q151N, Q151K, and K154A), and then the extension reactions were initiated by adding a trap mixture containing dNTPs, poly(rA)/oligodT, and heparin (see Materials and Methods). This condition allowed only a single round of primer extension by RT. All reactions were analyzed by 11% denaturing gel electrophoresis.

whereas it showed reduced processivity (<30 nt) with DNA template (Figure 5B). Changes in processivity of W153Y mutant protein were not observed (data not shown).

Inhibition of RT Activities of Q151 HIV-1 RT Mutants by AZTTP. The Q151M HIV-1 RT mutant is shown to possess AZT resistance. As many resistance mutations within HIV-1 RT have been mapped to the regions that interact with the template and incoming dNTPs (*10*, *25*), we investigated whether the two Q151 HIV-1 RT mutants isolated in this study also show an altered capability to distinguish AZTTP from natural dNTPs. The primer extension reactions with RNA and DNA templates were performed in the presence of either all dNTPs or mixtures of all dNTPs and AZTTP (Figure 6). The RT mutations rendering resistance to AZTTP (less incorporation of AZTTP) will produce larger amounts of fully extended primer (or less early terminated primer). Total RT activities of Q151 mutants used in these assays were lower (50% for RDDP and 90% for DDDP) than that of wild-type HIV-1 RT in order to confirm that the increase of fully extended products is due to less incorporation of AZTTP rather than a higher RT activity. As seen in Figure 6A and B, in the presence of AZTTP, wild-type HIV-1 RT showed a high level of early termination (use of AZTTP) at the sites with dA template sequence (* in Figure 6) and a lower level of fully extended products (arrow). This result indicates that wild-type HIV-1 RT is sensitive to AZTTP in both RDDP (Figure 6A) and DDDP activities (Figure 6B). Even with less total RT activities of the mutants added in the RDDP reaction (Figure 6A), Q151N showed much less early termination of the primer extension as well as a higher

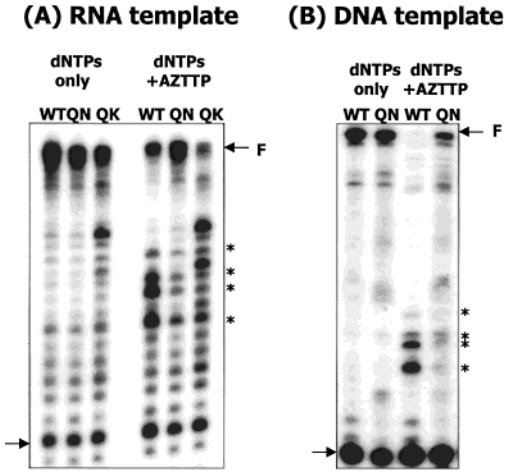

FIGURE 6: Inhibition of wild-type and Q151 mutant HIV-1 RT proteins by AZTTP in RDDP (A) and DDDP (B) reactions. The ^{32}P-labeled 17-mer primer (arrow) annealed to either 40-mer RNA (A) or 63-mer DNA (B) template was extended by wild-type HIV-1 RT, Q151N, and Q151K (only for RNA template) in the presence of only all four dNTPs (250 μM) or all dNTPs (250 μM) mixed with AZTTP (125 μM). In this assay, RT protein resistant to AZTTP produces a higher level of fully extended primer (arrow F) or a lower level of the primers terminated at the sites (*) where TTP or AZTTP can be incorporated. Two Q151 mutants used in this assay had 50% (Q151N) and 75% (Q151K) of wild-type HIV-1 RT activity.

level of fully extended products, compared to wild-type HIV-1 RT. This result indicates that the Q151N mutant is able to distinguish AZTTP from TTP. Unlike the Q151N mutant, Q151K (Figure 6A) showed significant inhibition by AZTTP.

DISCUSSION

Active sites of DNA polymerases interact with various molecules essential to the DNA polymerization reaction such as incoming dNTPs, template nucleotide base-pairing to the incoming dNTP, and the 3′ end primer nucleotide joining to the α-phosphate of the incoming dNTP. Unlike other DNA polymerases that use only DNA template exclusively, reverse transcriptases synthesize DNA from both DNA and RNA templates, which could require unique architectures in their active sites. Furthermore, unlike other high-fidelity reverse transcriptases such as AMV and MuLV RTs, the RT of HIV-1 that requires mutagenic DNA synthesis for evolutionary benefit could contain an even more unique local structure in its active site in order to be highly error-prone. It is also likely that functional or structural roles of the amino acid residues, even conserved between active sites of HIV-1 RT and other high-fidelity RTs, could be different. To elucidate the molecular strategies that HIV employs to build a highly mutagenic active site in its RT, we focused on biochemical characterization of HIV-1 RT mutants with altered fidelity. In this study, we isolated and biochemically characterized the fidelity of HIV-1 RT mutants which were constructed by structure-based site-directed mutagenesis.

Our recent studies with D76 and R78 HIV-1 RT high-fidelity (hi-fi) mutants (*15*, *16*) and other studies with Klenow fragment (*6*) and Taq Pol with altered fidelity (*7*) suggested that interactions of DNA polymerases with both template nucleotide and the incoming dNTP play important roles in determining the replication accuracy of DNA polymerases.

Based on these findings, we targeted the β8-αE loop of HIV-1 RT, which contains residues involved in the interaction with both the incoming dNTP and the template. In general, the targeted four amino acid residues in this loop region (Q151, G152, W153, and K154) lie at the bottom part of the HIV-1 RT active site connecting the fingers and palm domain, providing various interactions with the incoming dNTP and with two template nucleotides (Figure 1B). Other residues involved in catalysis, such as three conserved Asp residues (D113, D185, and D186), lie in the upper backside of the active site (Figure 1B), providing specific interactions with the phosphate part of the incoming dNTP and the 3′ end primer nucleotide to be joined to the incoming dNTP. As seen in the structure determined by Huang et al. (*10*), which represents only one step taken by the very flexible HIV-1 RT (Figures 1B and 7), residue Q151 interacts with the sugar of the incoming dNTP, and the main chain atoms of G152 lie directly under the sugar of the template nucleotide that base-pairs to the incoming dNTP. The K154 residue interacts with the phosphate group of the template nucleotide adjacent to the nucleotide base-pairing to the 3′ end primer nucleotide (not shown). Although the W153 residue does not directly interact with any of the HIV-1 RT substrate molecules, we mutated the W153 residue, expecting to alter the fidelity and biochemistry of the adjacent residues in the loop.

RT Activity. Among four mutated residues of the β8-αE region, Q151 and K154 mutants showed relatively high RDDP and DDDP activities. Q151N has high RT activities with all three DNA and RNA templates, whereas Q151K has relatively high RDDP activity, but only with heterogeneous RNA template. Surprisingly, the RDDP activity of Q151K was remarkably reduced with the poly(rA) template, which is one of the most preferred templates by wild-type HIV-1 RT. It is very likely that the structure of the wild-type HIV-1 RT dNTP binding pocket is locally malleable, and this dNTP binding site constantly modulates its structure depending on the properties of the templates, such as RNA, DNA, and their specific sequences. The larger Q151K mutation would alter the structure of the dNTP binding pocket much more than Q151N, which may affect the specific formation of the structure capable of incorporation of TTP during RDDP reaction from poly(rA) template. The four mutations in the G152 residue that interacts with the base and sugar moieties of the template nucleotide base-pairing to the incoming dNTP (*10*) completely inactivated RT activities. Presumably, adding any R group bigger than hydrogen at the G152 residue could directly alter the position of the template nucleotide base-pairing to the incoming dNTP. This alteration could interfere with proper alignment of the template nucleotide relative to the incoming dNTP for the base-pairing and cause failure of incorporation of the incoming dNTP. Two W153 mutations to smaller R groups, serine and alanine, lost RT activity, whereas W153Y had significant DDDP and RDDP activities. We also observed a much lower expression level of W153S and W153A proteins in *E. coli* than W153Y and wild-type proteins, which could be efficiently introducing a destabilizing hole into the structure.

Fidelity. In agreement with previous studies suggesting that direct interactions of DNA polymerases with the incoming dNTP and template play important roles in the accuracy of DNA synthesis, we found that several HIV-1 RT mutants obtained in this study targeting the β8-αE region showed altered fidelity.

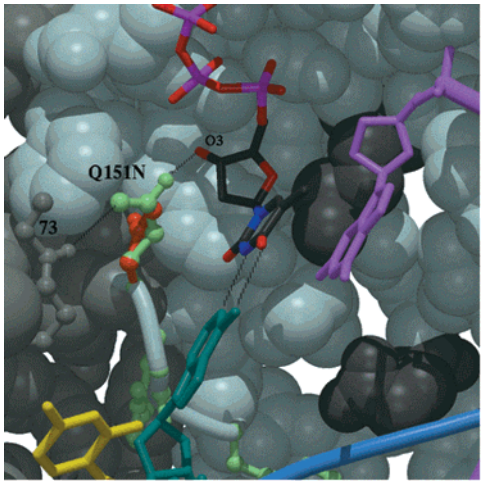

FIGURE 7: Interaction of Q151 and N151 residues at the β8-αE region of HIV-1 RT with incoming dNTP. This figure shows the interactions of wild-type Gln (light green) with O3 of the sugar moiety of the incoming TTP and the Lys residue at position 73 (gray) near the catalytic site of HIV-1 RT complexed with template, primer, and incoming nucleotide (*10*) using coordinate set 1rtd.pdb from the Protein Data Bank (*32*). The Asn mutation at 151 is shown in orange. Asn has a shorter R side chain than Gln, and cannot form interactions with either the sugar of the incoming TTP or the backbone carboxyl oxygen at position 73. The single-strand part of the template is shown in yellow. The primer nucleotide at its 3′ end is purple, the incoming dNTP is red−black, and the nucleotide base-paired to the incoming nucleotide is blue−green. The double-stranded part of the template annealed to the primer nucleotide is light blue. The finger domain is shown in a dark gray space-filling representation, and the palm domain containing E89 (black) and M184 (black) in a light gray space-filling representation. This figure was made using the programs Molscript (*33*) and Raster3D (*34*).

First, as seen in the misincorporation assay and the M13 lacZ forward mutation assay, the Q151N mutation enhanced replication accuracy. The Q151K mutant also showed reduced misincorporation in the reaction with RNA template. As seen in Figure 2, the Q151N mutant showed a much lower level of total primer extended beyond the stop sites than wild-type HIV-1 RT in the reactions with four different kinds of biased dNTP pools. This indicates that the Q151N mutant has less capability to incorporate incorrect dNTPs at the stop sites compared to wild-type HIV-1 RT. Furthermore, the experiment shown in Figure 4 demonstrated that the Q151N mutant is also much less capable of the extension of the mismatched primer, which is the second step in the synthesis of a single mutation.

Examination of the structure shows that $O^{\epsilon 1}$ of the Q151 residue in wild-type HIV-1 RT interacts with O3 of the sugar moiety of the incoming correct dNTP (Figure 7, *10*). This Q151 interaction with the incoming dNTP, together with proper base-pairing between the incoming dNTP and template nucleotide, could be a major element for efficient formation of the RT−dNTP−T/P complex that is an intermediate of the DNA polymerization reaction. It is plausible that the Q151 residue could also make the interaction with the sugar of the incorrect dNTP efficiently, and that this interaction may become a dominant factor for incorporation of incorrect dNTP in the case of wild-type HIV-1 RT with low fidelity. In other words, the Q151 interaction with incorrect dNTP might be sufficient for

holding the incorrect dNTP in the catalytic site long enough to execute the DNA polymerization reaction even in the absence of the proper base-pairing between the incorrect dNTP and the template nucleotide. However, it is likely that the Q151N mutant, with its shorter side chain, might lose the interaction with O3 of the sugar moiety of the incoming dNTP (Figure 7). In the absence of the RT interaction with the sugar of the incoming dNTP, the base-pairing between the incoming dNTP and template nucleotide becomes the primary remaining determinant for incorporation of dNTPs. Therefore, in the reaction with the Q151N mutant, the correct dNTP with stable base-pairing with template nucleotide is still able to be incorporated as shown by high RT activity of the Q151N mutant (Table 1). In contrast, the incorrect dNTP lacking both proper base-pairing with template nucleotide and interaction of the 151 residue could not be held stably enough to be incorporated. This results in reduction of misincorporation (the first step of the mutation synthesis) and enhancement of accuracy of DNA polymerization. Furthermore, the data presented in Figure 4 show that the Q151N mutant has a reduced capability to extend mismatched primers. Thus, the Q151 interaction with the incoming dNTP could also play a critical role in incorporation of dNTP at the 3′ mismatched end of the primer (i.e., the second step of the mutation synthesis). It is very likely that mismatch at the 3′ end of the primer alters the geometry between the α-phosphate of the incoming dNTP and the 3′-OH of the primer nucleotide, causing difficulty in the incorporation of the incoming correct dNTP next to the mismatch and enhancing the accuracy of DNA polymerization. In wild-type HIV-1 RT with low fidelity, however, this difficulty can be efficiently overcome by the interaction between Q151 and the next incoming dNTP, allowing the extension of the mismatched primer and completion of the mutation synthesis. Therefore, in the case of the Q151N mutant, with loss of the interaction with the incoming dNTP, base-pairing between the incoming dNTP and template nucleotide is the only remaining element holding the incoming dNTP in the active site. This base-pairing, which was enough by itself to incorporate the correct dNTP at the 3′ end of matched primer in wild-type RT, is presumably insufficient to execute the incorporation of the dNTPs at the 3′ end of the mismatched primer (Figure 3), resulting in failure of completion of the second step of the mutation synthesis, and enhancement of fidelity. Alternatively, the fidelity increase of Q151 mutations may result from changes in other factors such as catalysis, binding to mismatched template-primer, and the structure of RT. In addition, it has been shown that the mutation frequency of HIV RT varies with the sequence context of the RNA or DNA template (*26*, *27*). It is also possible that the fidelity changes by Q151 mutations are template/sequence-specific. These alternatives can be further tested by kinetic and structural analyses with the Q151 mutants.

Interestingly, Q151K showed a higher level of misincorporated primer at the stop sites, compared to Q151N (* in Figure 2), indicating that Q151K is still capable of misincorporation (first step of mutation synthesis), like wild-type HIV-1 RT.

We also found that the K154A mutant showed only a 2.1-fold higher fidelity than wild type. We recently showed that mutations at two residues of HIV-1 RT, D76 and R78, enhanced fidelity 8.8- and 9-fold, respectively. These two residues lie near the phosphate group of the template nucleotide that base-pairs to the incoming dNTP (Figure 1B), whereas K154 directly interacts with the phosphate of the template nucleotide adjacent to the nucleotide that base-pairs to the 3′ end primer template (Figure 1B). As shown in the E89G mutant with increased fidelity, it was suggested that interaction with the penultimate nucleotide of double-stranded RNA or DNA templates is also important for RT fidelity (*17*). Even if the effect of the K154A mutant on RT fidelity is relatively small, this finding additionally supports the view that interaction of HIV-1 RT with the template nucleotides may play an important role in the accuracy of DNA synthesis.

Drug Resistance. As predicted by the resistance of Q151M containing HIV mutants to dideoxynucleotide analogues such as AZT (*11*, *12*), we also found that the Q151N mutant showed a much reduced level of incorporation of AZTTP, which is a TTP analogue with an altered sugar moiety (Figure 6). As discussed above, residue Q151 of HIV-1 RT interacts with the sugar moiety of the incoming dNTP (*10*). Specifically O3 of the ribose is poised between $O^{\epsilon 1}$ of Q151 and the peptide nitrogen of Y115. Q151 is further anchored by a hydrogen bond between $N^{\epsilon 2}$ and the carbonyl oxygen of K73 (Figure 7). There are no specific hydrogen bonds to the incoming base other than those from the template. Q151 is very close to making contacts (3.5 Å) with R72 (not shown in Figure 7, as it lies directly between the viewer and residue 151) which in turn hydrogen bonds to the incoming nucleotide phosphate. Taken together, these three residues (Q151, R72, and Y115) seem to make a cage in which hydrogen bonding between incoming nucleotides and template can happen. In the dideoxy NTP RT inhibitors, O3 is absent, which could free up Q151 for more specific interactions—perhaps stronger interactions with R72, or new specific interactions with the base itself. For example, it is known that wild-type Taq Pol that has been extensively used for PCR-based DNA sequencing prefers incorporation of ddGTP, which results in uneven sequencing signals (*9*, *28*). This is explained by the crystal structure of Taq Pol in complex with ddGTP. In this structure, unlike Taq Pol structures with other ddNTPs, Arg660 of Taq Pol forms additional hydrogen bonds with the base of the incoming ddGTP, thereby explaining the preferential utilization of ddGTP (*9*, *28*). Mutations at Arg660 of Taq Pol also reduced the incorporation of ddGTP chain terminator, which results in even DNA sequencing signals (*9*). Thus, the Q151 residue of wild-type HIV-1 RT might also have additional interaction(s) with incoming AZTTP that contains three nitrogens of the azido group in the place of O3 of ribose, thereby explaining the high incorporation of AZTTP by wild-type HIV-1 RT (sensitivity to AZTTP). In contrast, the Q151N mutant could cause loss of the interaction(s) specific for AZTTP, thereby reducing incorporation of AZTTP. Interestingly, unlike the Q151N mutant, the Q151K mutant showed relatively high sensitivity to AZTTP, suggesting that a Lys residue at position 151 might be able to provide similar interactions specific for AZTTP to those provided by the Gln residue of wild-type HIV-1 RT.

Processivity. We also found that mutations in the β8-αE loop affect processive DNA synthesis by HIV-1 RT. Our recent studies with D76 and R78 HIV-1 RT hi-fi mutations

showed that alterations in the RT interaction with template affect the processivity as well as fidelity (*16*). As seen in Figure 5, mutations at the K154 residue, which also interacts with the template nucleotide base-pairing to the primer nucleotide at the 3′ end (Figure 1 B), result in reduced enzymatic processivity in DDDP even though no distinct difference was observed in processivity with poly(rA) template. Presumably, residue K154 of HIV-1 RT plays an important role in processive DNA synthesis from a DNA template.

It was not expected that Q151 mutations (i.e., mutations in the dNTP binding residues) could affect processivity because a relationship between dNTP binding and processivity of DNA polymerases has not been demonstrated. All HIV-1 RT mutants with altered fidelity have altered interactions with either template [D76V (*16*), R78A (*15*)] or primer [M184I (*29*) and primer grip mutants (*30*, *31*)]. Like the R78 HIV-1 RT mutant, Q151 mutants have both increased fidelity and reduced processivity. It is possible that structural changes in the dNTP binding site caused by Q151 mutations may destabilize the binding of the incoming dNTP. This could lead to frequent pausing of HIV-1 RT during DNA polymerization and release of RT from the template, which results in reduction of its processivity. Q151K might induce a much larger structural change in the dNTP binding site than the Q151N mutant, as indicated by the larger reduction of its specific activity. It is also possible that the decrease of processivity by Q151 mutations could be due to lower binding affinity of these mutants.

Residue Q151 is conserved in high-fidelity RTs, such as MuLV RT (Q189), indicating that the role of the HIV-1 RT Q151 interaction with the incoming dNTP in fidelity could be unique. As shown in this study, the Q151 residue of HIV-1 RT is responsible for its poor ability to distinguish correct vs incorrect dNTPs. However, this mutagenic function of the Gln residue observed in HIV-1 RT might be absent in the high-fidelity RTs, which makes them much less error-prone than HIV-1 RT. This possibility predicts that, unlike Q151 of HIV-1 RT, Q189 of MuLV RT does not have any specific interactions with incorrect dNTP. Therefore, this possibility also predicts that mutations in the Gln residues of the high-fidelity RTs cannot increase their fidelity further. Similar discrepancies in the roles of residues conserved between HIV-1 RT and other high-fidelity RTs have been observed previously. For example, mutations in residue R78 in the finger domain of HIV-1 RT increase fidelity 9-fold. This Arg residue is also conserved as residue R116 in the MuLV RT's finger domain. In contrast to DDDP and RDDP activities of HIV-1 RT R78A mutant which are similar to those of wild-type HIV-1 RT, R116A MuLV RT totally loses both DDDP and RDDP activities (our unpublished data). This suggests that R116 of MuLV RT is much more essential to its RT activity than the R78 residue of HIV-1 RT is to HIV-1 RT activity. Therefore, it is possible that even mutations in amino acid sequences that are conserved between HIV-1 RT and MuLV RT may affect their RT's biochemical properties in different ways. Therefore, it is plausible that the mutagenic role of the conserved Gln residue occurs only in HIV-1 RT.

It is likely that HIV-1 employs several molecular strategies to establish a highly mutagenic active site in its RT. In addition to our recent findings with D76 and R78 hi-fi mutants and other studies with Taq Pol and Klenow fragment, this study confirms that the residues in the β8-αE loop region of HIV-1 RT interacting with the incoming dNTP (Q151) and template nucleotide (K154) play important roles in the accuracy of DNA synthesis and the utilization of nucleotide analogue RT inhibitors.

ACKNOWLEDGMENT

We thank Drs. Robert A. Bambara, Daksha Patel, Stephen Dewhurst, and Ann Blank for critical reading of the manuscript.

REFERENCES

1. Preston, B. D., Poiesz, B. J., and Loeb, L. A. (1988) *Science 242*, 1168−1171.
2. Williams, K. J., and Loeb, L. A. (1992) *Curr. Top. Microbiol. Immunol. 176*, 165−180.
3. Coffin, J. M. (1995) *Science 267*, 483−489.
4. Coffin, J. M. (1990) Retroviridae and Their Replication. in *Virology* (Fields, B. N., Knipe, D. M., Chanock, R. M., et al., Eds.) pp 1437−1500, Raven, New York.
5. Roberts, J. D., Preston, B. D., Johnston, L. A., Soni, A., Loeb, L. A., and Kunkel, T. A. (1989) *Mol. Cell. Biol. 9*, 469−489.
6. Minnick, D. T., Bebenek, K., Osheroff, W. P., Turner, R. M., Jr., Astatke, M., Liu, L., Kunkel, T. A., and Joyce, C. M. (1999) *J. Biol. Chem. 274*, 3067−3075.
7. Suzuki, M., Avicola, A. K., Hood, L., and Loeb, L. A. (1997) *J. Biol. Chem. 272*, 11228−11235.
8. Beese, L. S., Friedman, J. M., and Steitz, T. A. (1993) *Biochemistry 32*, 14095−14101.
9. Li, Y., Mitaxov, V., and Waksman, G. (1999) *Proc. Natl. Acad. Sci. U.S.A. 96*, 9491−9496.
10. Huang, H., Chopra, R., Verdine, G. L., and Harrison, S. C. (1998) *Science 282*, 1669−1675.
11. Villalba, N., Gomez-Cano, M., Holguin, A., and Soriano, V. (1999) *Eur. J. Clin. Microbiol. Infect. Dis. 18*, 372−375.
12. Harris, D., Kaushik, N., Pandey, P. K., Yadav, P. N., and Pandey (1998) *J. Biol. Chem. 273*, 33624−33634.
13. Rezende, L. F., Curr, K., Ueno, T., Mitsuya, H., and Prasad, V. R. (1998) *J. Virol. 72*, 2890−2895.
14. Carroll, S. S., Cowart, M., and Benkovic, S. J. (1991) *Biochemistry 30*, 804−813.
15. Kim, B., Hathaway, T. R., and Loeb, L. A. (1998) *Biochemistry 37*, 5831−5839.
16. Kim, B., Ayran, J. C., Sagar, S. G., Adman, E. T., Fuller, S. M., Tran, N. H., and Horrigan, J. (1999) *J. Biol. Chem. 274*, 27666−27673.
17. Drosopoulos, W. C., and Prasad, V. R. (1996) *J. Virol. 70*, 4834−4838.
18. Kim, B., Hathaway, T. R., and Loeb, L. A. (1996) *J. Biol. Chem. 271*, 4872−4878.
19. Kim, B. (1997) *Methods 12*, 318−324.
20. Battula, N., and Loeb, L. A. (1974) *J. Biol. Chem. 249*, 4086−4093.
21. Bebenek, K., and Kunkel, T. A. (1995) *Methods Enzymol. 262*, 217−232.
22. Varatnian, J. P., Meyerhans, A., Asjo, B., and Wainhobson, S. (1991) *J. Virol. 65*, 1779−1789.
23. Fitzgibbon, J. E., Mazar, S., and Dubin, D. T. (1993) *AIDS Res. Hum. Retroviruses 9*, 833−838.
24. Huber, H. E., McCoy, J. M., Seehra, J. S., and Richardson, C. C. (1989) *J. Biol. Chem. 264*, 4669−4678.
25. Ding, J., Das, K., Tantillo, C., Zhang, W., Clark, A. D., Jr., Jessen, S., Lu, X., Hsiou, Y., Jacoba-Molina, A., Andries, K., Pauwels, R., Moereels, H., Koymans, L., Janssen, P. A. J., Smith, R. H., Jr., Koepke, M. K., Michejda, C. J., Hughes, S. H., and Arnold, E. (1995) *Structure (London) 3*, 365−379.
26. Yu, H., and Goodman, M. F. (1992) *J. Biol. Chem. 267*, 10888−10896.
27. Ji, J. P., and Loeb, L. A. (1992) *Biochemistry 31*, 954−958.
28. Li, Y., Korolev, S., and Waksman, G. (1998) *EMBO J. 17*, 7514−7525.

29. Miller, M. D., Lamy, P. D., Fuller, M. D., Mulato, A. S., Margot, N. A., Cihlar, T., and Cherrington, J. M. (1998) *Mol. Pharmacol. 54*, 291−297.
30. Bebenek, K., Beard, W. A., Casas-Finet, J. R., Kim, H.-R., Darden, T. A., Wilson, S. H., and Kunkel, T. A. (1995) *J. Biol. Chem. 270*, 19516−19523.
31. Wisniewski, M., Palaniappan, C., Fu, Z., Le Grice, S. F., Fay, P., and Bambara, R. A. (1999) *J. Biol. Chem. 274*, 28175−28184.
32. Bernstein, F. C., Koetzle, T. F., Williams, G. J. B., Meyer, E. F., Bruce, M. D., Rodgers, J. R., Kennard, O., Shimanouchi, T., and Tasmui, M. (1977) *J. Mol. Biol. 112*, 535−542.
33. Kraulis, P. (1991) *J. Appl. Crystallogr. 24*, 946−950.
34. Merritt, E. A., and Bacon, D. J. (1997) *Methods Enzymol. 277*, 505−524.

BI000788Y